

# Systematical Analyses of Proton-Nuclei Scattering with the Relativistic Microscopic Optical Potential\*

Ma Zhongyu, Gu Yingqi, Zhu ping and Zhuo Yizhong

(Institute of Atomic Energy, Beijing)

---

The relativistic microscopic optical potential (RMOP) of a nucleon above the Fermi sea based on the Walecka's model is used to systematically analyze the proton elastic scattering from nuclei for a variety of energies. It turns out that the experimental data of the differential cross sections, the analyzing powers and the spin rotation functions are reproduced satisfactorily except for large angles. This simple model might be used in the nuclear transport theory and heavy ion collision and to take account of both the nuclear medium and relativistic effects.

---

## 1. INTRODUCTION

Recently more and more extensive and precise measurements have been made for the elastic scattering of the proton from nuclei over broad ranges of proton energy and target mass. These experiments include not only measurements of the differential cross sections but also spin observable, such as the analyzing powers and the spin rotation functions. These accurate experimental data have provided more information about the nucleon-nucleus interaction, which can help to remove partly the ambiguity of the nuclear potential, to critically check the microscopic nuclear optical potential in terms of a two-body nucleon-nucleon interaction and to extract the effect of the nuclear medium and other effects.

In the early 1980's, the success of the Dirac phenomenology [2] and the relativistic impulse approximation [3] in explaining and predicting the detailed structure of the spin

---

\* Supported by the National Natural Science Foundation of China.

Received on August 11, 1987

observable for the proton-nucleus elastic scattering at high energies has aroused people's great interest in investigating the relativistic effects in nuclear physics. Our previous work [1] calculated the relativistic microscopic optical potentials in the framework of the Walecka's model[4] with the effective Lagrangian density including nucleon, sigma and omega mesons only to investigate both the relativistic and nuclear medium effects, because the effect of the nuclear medium is important at  $E < 300$  MeV and cannot be neglected. In the nuclear medium the effective meson-nucleon couplings  $g_\sigma$  and  $g_\omega$  are adjusted by reproducing the nuclear matter saturation properties in the relativistic Hartree-Fock approximation (RHFA). In our calculations the real part of the optical potential is taken from the Hartree-Fock self-energy of a nucleon in the nuclear matter and the imaginary part is calculated by the second order Feymann diagram of the self-energy. A local RMOP for a finite nucleus can be obtained by the local density approximation (LDA). In this paper we systematically analyze the experimental data of the proton-nucleus elastic scattering, such as differential cross sections,  $d\sigma/d\Omega$  analyzing powers  $P(\theta)$  and spin rotation functions  $Q(\theta)$ . The theoretical calculations are in full agreement with the experimental data. In the region of the forward scattering with  $\theta < 70^\circ$  the results not only reproduce the differential cross sections quite well, but also give the detailed structures of the spin observable. The comparisons of the RMOP with the phenomenological ones are also given in this paper. It can be seen that the real parts of both potentials are rather similar. But the difference of the imaginary parts is quite large and they even have different Lorentz structures, which shows the ambiguities of the imaginary optical potentials.

The results show that the RMOP based on the Walecka's model in the lowest order approximation is suitable in describing the proton-nucleus elastic scattering for various target nuclei and a wide energy range  $Ep < 300$  MeV. This simple model might be used in the nuclear transport theory and heavy ion reaction and to take account of both the nuclear medium and relativistic effects.

## 2. NUCLEON-NUCLEUS EFFECTIVE INTERACTION

We start from an effective Lagrangian density including nucleon, isoscalar mesons  $\sigma$  and  $\omega$ ,

$$\begin{aligned} \mathcal{L} = & \bar{\psi}(i\gamma^\mu \partial_\mu - M)\psi + \frac{1}{2}(\partial^\mu \sigma \partial_\mu \sigma - m_\sigma^2 \sigma^2) + \frac{1}{2}m_\omega^2 \omega_\mu \omega^\mu \\ & - \frac{1}{4}F^{\mu\nu}F_{\mu\nu} - g_\sigma \bar{\psi}\sigma\psi - g_\omega \bar{\psi}\gamma^\mu \omega_\mu \psi \end{aligned} \quad (2.1)$$

with  $F_{\mu\nu} = \partial_\mu \omega_\nu - \partial_\nu \omega_\mu$ , where  $\psi$ ,  $\sigma$ ,  $\omega_\mu$  are the field operators of the nucleon,  $\sigma$  and  $\omega$  mesons respectively.  $M$ ,  $m_\sigma$ ,  $m_\omega$  are their corresponding masses and  $M = 938.9$  MeV,  $m_\sigma = 550$  MeV,  $m_\omega = 783$  MeV are taken in our calculations. The effective meson-nucleon coupling constants in the nuclear medium  $g_\sigma$  and  $g_\omega$  are adjusted by reproducing the saturation properties of the nuclear matter, i.e. the nuclear matter is saturated at  $k_F = 1.36 \text{ fm}^{-1}$  and the binding energy per nucleon is 15.75 MeV. One obtains that  $g_\sigma^2/4\pi = 7.3$ ,  $g_\omega^2/4\pi = 10.9$ .

The nucleon self-energy caused by the meson exchanges in the nuclear matter can be written, in general, as

$$\Sigma(k_\nu, k_F) = \Sigma^s(k_\nu, k_F) - \gamma^0 \Sigma^0(k_\nu, k_F) + \underline{\gamma} \cdot \underline{k} \Sigma^v(k_\nu, k_F), \quad (2.2)$$

where  $\Sigma^s$ ,  $\Sigma^0$ ,  $\Sigma^v$ , are the scalar self-energy, the time and space components of the vector self-energy respectively. Generally, they are functions of the four-dimension momentum  $k_\nu$  of a nucleon and the density  $k_F$  of the nuclear matter.

In the lowest order approximation the real part of the nucleon self-energy above the Fermi sea is the Hartree-Fock contribution and the lowest order contribution to the imaginary part of the nucleon self-energy comes from the second order diagram, i.e. the core polarization diagram. It is known that the self-energy of a nucleon in the nuclear medium is identified with the nucleon-nucleus effective interaction, namely, the nuclear optical potential.

The local RMOP for a finite nucleus  $\Sigma(r, E)$  is a function of nucleon energy and can be obtained by the local density approximation (LDA). The wave function of a nucleon obeys the Dirac type equation,

$$[\alpha \cdot p(1 + \Sigma^v) + \gamma^0(M + \Sigma^s) - \Sigma^0]\psi = E\psi \quad (2.3)$$

By rearranging the above equation, a new form of the Dirac equation with scalar and vector potentials only is obtained as follows:

$$[\alpha \cdot p + \gamma^0(M + U_s) + U_0]\psi = E\psi, \quad (2.4)$$

where

$$U_s = \frac{\Sigma^s - \Sigma^v M}{1 + \Sigma^v}, \quad U_0 = \frac{-\Sigma^0 + E \Sigma^v}{1 + \Sigma^v}.$$

To calculate the scattering amplitude of the nucleon-nucleus elastic scattering one obtains the Schrödinger type equation for the large components of the Dirac wave function by eliminating the small component,

$$\left[ p^2 + i \frac{1}{D(r)} \frac{d}{dr} D(r) \hat{r} \cdot \underline{p} - \frac{1}{D(r)} \frac{dD(r)}{dr} \frac{\underline{\sigma} \cdot \underline{L}}{r} + D(r) G(r) \right] \psi_> = 0. \quad (2.5)$$

where

$$\begin{aligned} D(r) &= M + U_s(r) + E - U_0(r) - V_c(r) \\ G(r) &= M + U_s(r) - E + U_0(r) + V_c(r) \end{aligned}$$

and  $V_c$  is the Coulomb potential. In order to remove the first derivative term one introduces the following transformation,

$$\psi_>(r) = \sqrt{\frac{D(r)}{M + E}} \varphi(r). \quad (2.6)$$

$\psi > (r) = \varphi(r)$  at  $r \rightarrow \infty$ , i.e. they have exactly the same asymptotic behavior. Thus, the Schrödinger type equation of the wave function is obtained,

$$\left[ \frac{p^2}{2E} + U_{cen}(r) + V_c(r) + U_{LS}\sigma \cdot L \right] \varphi(r) = \frac{E^2 - M^2}{2E} \varphi(r) \quad (2.7)$$

where the central and spin-orbit coupling potentials of the Schrödinger equivalent potentials are as follows, respectively,

$$\begin{aligned} U_{cen}(r) &= U_0 + \frac{1}{2E} [U_s(2M + U_s) - (U_0 + V_c)^2] \\ &+ \frac{1}{2E} \left[ -\frac{1}{2r^2 D(r)} \frac{d}{dr} \left( r^2 \frac{dD(r)}{dr} \right) + \frac{3}{4} \left( \frac{1}{D(r)} \frac{dD(r)}{dr} \right)^2 \right] \\ U_{LS}(r) &= -\frac{1}{2ErD(r)} \frac{dD(r)}{dr}. \end{aligned}$$

The third term of the central potential, called the Darwin term, is small and negligible.

The Schrödinger equivalent potentials for the  $p + {}^{40}\text{Ca}$  scattering at different incident energies are calculated. The calculation shows that the depths of the central real potentials decrease and the potentials are changed from being attractive to repulsive, as the energy increases. At the intermediate energy around  $E_p = 200$  MeV an attractive pocket is found at the nuclear surface. This is the so called "wine bottle bottom" shape. The central imaginary potentials are mainly surface absorption below several tens of MeV and become volume dominant as the energy increases. The spin-orbit coupling potentials can be directly obtained from the Dirac equation. They are surface-peaked and the strength decreases for the real part and increases for the imaginary part as the energy increases. These features are very similar to that of the phenomenological potentials.

### 3. PROTON-NUCLEUS ELASTIC SCATTERING

The calculations of the RMOP are performed for nuclear matter. The local RMOP for a finite nucleus is obtained by the LDA. In other words, the RMOP at point  $r$  for a finite nucleus is calculated by the RMOP in the nuclear matter which has the same density as the finite nucleus at  $r$ . The density distributions of nuclei are taken from the Negele's empirical formula [5], except for light nuclei, such as  ${}^{12}\text{C}$ ,  ${}^{16}\text{O}$ ,

$$\rho(r) = \frac{\rho_0}{1 + \exp[(r - c)/a]} \quad (3.1)$$

where  $\rho_0$  is determined by the normalization,

$$\rho_0 = \frac{3A}{4\pi c^3(1 + \pi^2 a^2/c^2)}$$

here  $a = 0.54$  fm,  $c = (0.978 + 0.0206 A^{1/3}) A^{1/3}$  fm, and  $A$  is the nucleon number of the target. The Gaussian type density distributions are chosen for  ${}^{12}\text{C}$ ,  ${}^{16}\text{O}$  [6],

$$\rho(r) = \rho_0(1 + \alpha r^2/a^2) \exp\left(-\frac{r^2}{a^2}\right)$$



$$\rho_0 = \frac{A}{4\pi a^3} \sqrt{\pi} \left( \frac{1}{4} + \frac{3}{8} \alpha \right) \quad (3.2)$$

where  $\alpha$  and  $a$  are taken as 4/3 and 1.65 fm for  $^{12}\text{C}$ ; and 2 and 1.76 fm for  $^{16}\text{O}$ , respectively.  
 The amplitude of the proton scattering from a zero-spin nucleus can be expressed by the spin dependent and spin independent parts,

$$F(\theta) = A(\theta) + \sigma \cdot \hat{n} B(\theta) \quad (3.3)$$

where  $\sigma$  is the spin operator of the proton,  $\hat{n}$  is the unit vector perpendicular to the

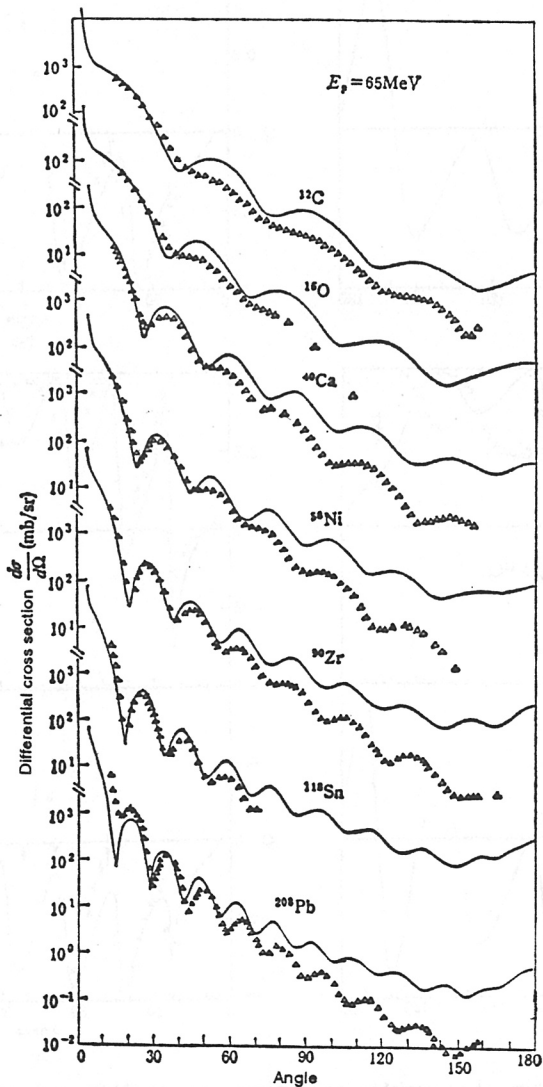


**FIG. 1** The differential cross sections of the proton elastic scattering from a set of spherical target nuclei at  $E_p = 65$  MeV.

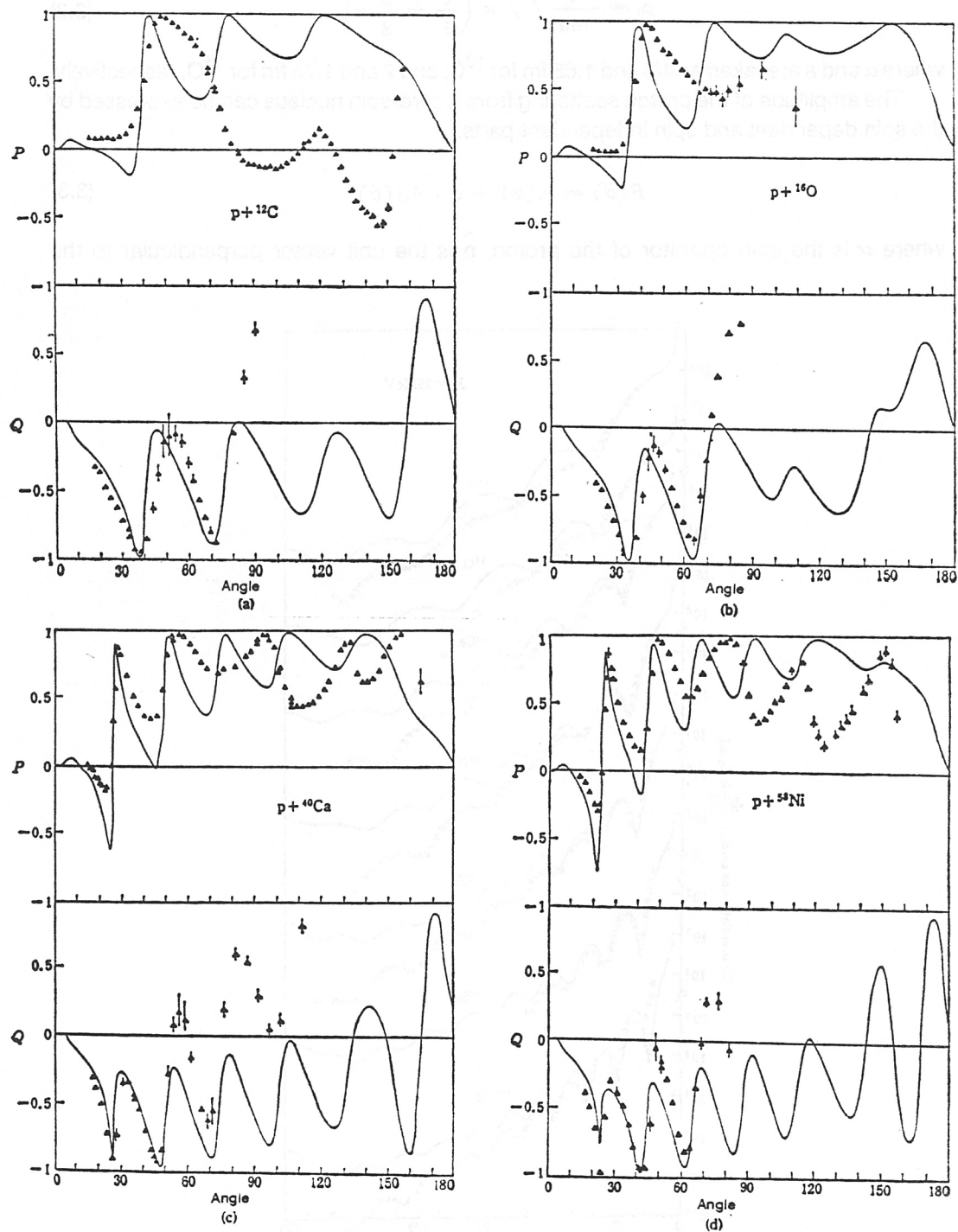


FIG. 2 The spin observable, analyzing power  $P(\theta)$  and spin rotation functions  $Q(\theta)$  of the proton elastic scattering from spherical nuclei at  $E_p = 65$  MeV.

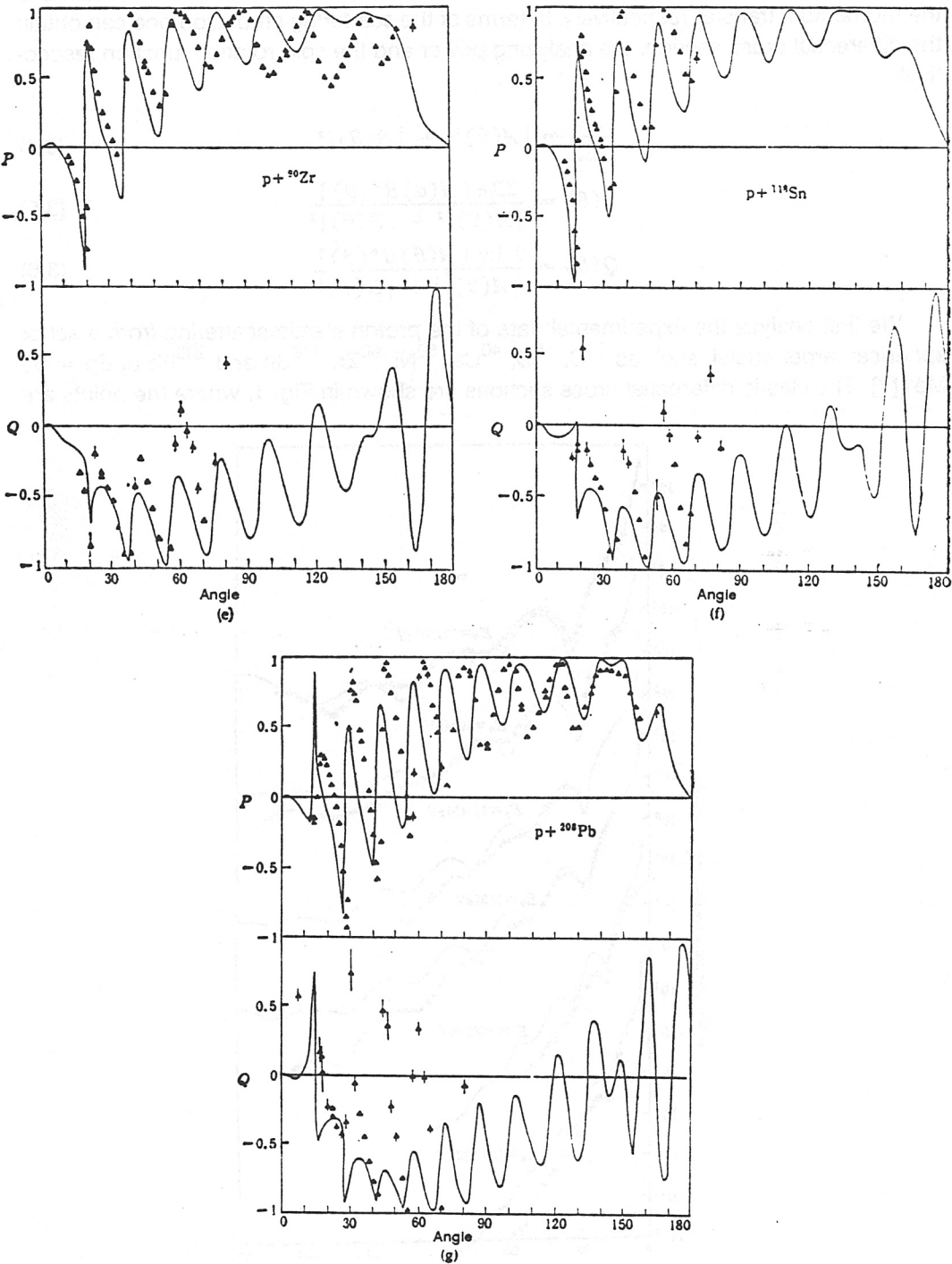


FIG. 2  
Continued

scattering plane,  $\hat{n} = \hat{k} \times \hat{q}$ ,  $\hat{k}$  and  $\hat{q}$  are the unit vectors of the incident momentum and the momentum transfer respectively. In terms of the scattering amplitude one can obtain the differential cross section, the analyzing power and the spin rotation function respectively,

$$\frac{d\sigma}{dQ} = |A(\theta)|^2 + |B(\theta)|^2 \quad (3.4)$$

$$P(\theta) = \frac{2\text{Re}[A(\theta)B^*(\theta)]}{|A(\theta)|^2 + |B(\theta)|^2} \quad (3.5)$$

$$Q(\theta) = \frac{2\text{Im}[A(\theta)B^*(\theta)]}{|A(\theta)|^2 + |B(\theta)|^2} \quad (3.6)$$

We first analyze the experimental data of the proton elastic scattering from a set of spherical target nuclei, such as  $^{12}\text{C}$ ,  $^{16}\text{O}$ ,  $^{40}\text{Ca}$ ,  $^{58}\text{Ni}$ ,  $^{90}\text{Zr}$ ,  $^{118}\text{Sn}$  and  $^{208}\text{Pb}$  at  $E_p = 65$  MeV[7]. The elastic differential cross sections are shown in Fig. 1, where the points are

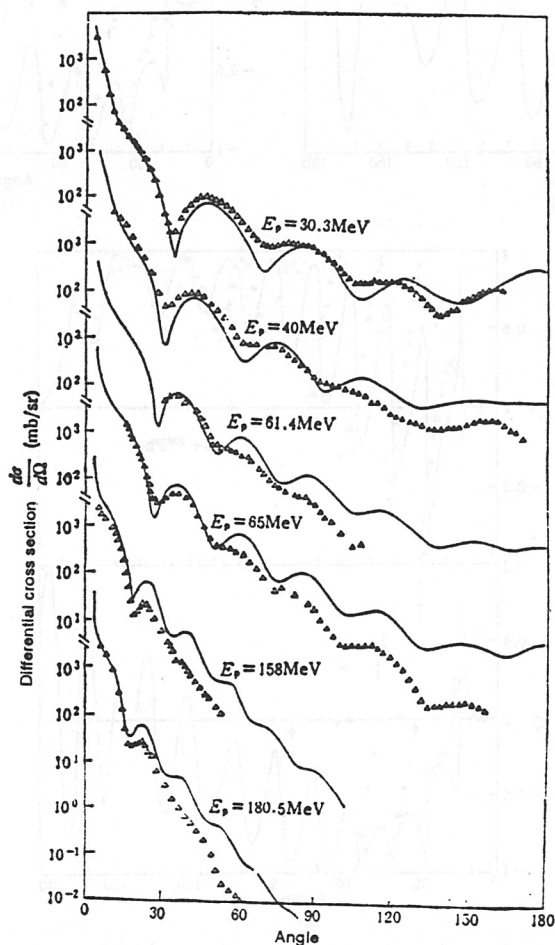


FIG. 3 The differential cross sections of  $p + ^{40}\text{Ca}$ . The experimental data are taken from Ref.[8].

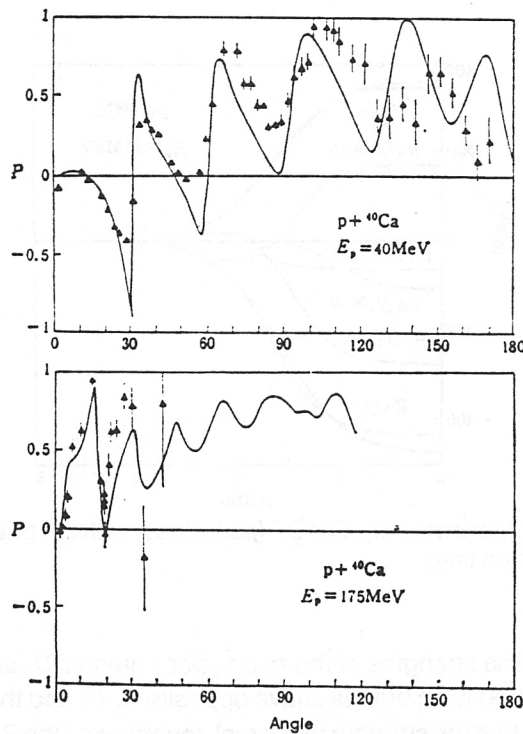


FIG. 4 The analyzing powers of  $p + {}^{40}\text{Ca}$ . [8]

the experimental values and the solid lines are the theoretical results in terms of the RMOP. It is found that the theoretical calculations can reproduce the experimental diffraction pattern. At the forward angles  $\theta < 70^\circ$  the agreement of the theoretical results with the experiments is quite satisfactory. At the backward angles the theoretical values are overestimated. The spin observable, the analyzing powers and the spin rotation functions are shown in Fig. 2. The agreement of the theoretical result with the experiments is similar to that for the differential cross sections. The calculations can describe the detailed structure of the spin observable at small angles and deviate from the experiments at large angles. The scattering at large angles, i.e. with a large momentum transfer, are mainly determined by the interior structure of the nuclear potential, we have adopted the empirical density and LDA for a finite nucleus used in our calculations, which can not give the detailed structure of the nuclear density distribution and the nonlocal properties of the nuclear potentials.

We also analyze the experimental data of the proton elastic scattering from  ${}^{40}\text{Ca}$  with a variety of incident energies. The differential cross sections and analyzing powers for the incident energies from 30 MeV to 180 MeV are given in Figs.3 and 4. Due to the lack of the experimental data, the results of the spin rotation functions have not been shown here.

To investigate the properties of the nuclear potentials, the comparisons of the RMOP with the phenomenological potentials [9] are made. The  $p + {}^{40}\text{Ca}$  scattering at  $E_p = 65$  MeV is taken as an example and the results are shown in Fig. 5. It shows that their real



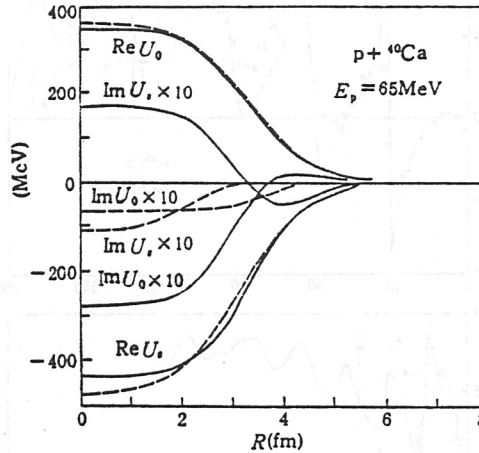


FIG. 5 The comparison of the RMOP (solid lines) with the phenomenological ones (dashed lines).

parts are very similar. The strengths of the real scalar potential  $U_s$  and vector potential  $U_0$  are about several hundred MeV, but they have opposite signs and the cancellation of each other results in the fact that the strength of the real central parts the Schrödinger equivalent potential is about several tens of MeV. Their variations with respect to the radial variable  $r$  are summed up and produce naturally the real part of spin-orbit potential. In contrast, the imaginary parts of the RMOP and the phenomenological potentials are quite different and they even have different Lorentz structures. It should be pointed out that the imaginary parts of the phenomenological potentials have some ambiguities. The one given by Clark et al. [10] is similar to ours and has the same Lorentz structures as ours. Due to the different Lorentz structures, the imaginary part of the central potential of the Schrödinger equivalent potential for the phenomenological one [9] is obtained by adding the imaginary parts of the scalar and vector potentials. The imaginary spin-orbit potentials are negative and opposite to the microscopic ones in sign. Since the imaginary spin-orbit potentials are very small at low energies, such as  $E_p = 65$  MeV, it has little influence on the results.

#### 4. DISCUSSION

Based on the Walecka's model and starting from an effective Lagrangian density with the sigma and omega mesons only we have calculated the RMOP in the lowest order approximations. The systematical analyses of the proton elastic scattering from a variety of spherical target nuclei, from  $^{12}\text{C}$  to  $^{208}\text{Pb}$ , with the incident proton energies below 200 MeV have been made in this work. The theoretical results are in full agreement with the experimental data. Our calculations reproduce the differential cross sections and describe the detailed structures of the spin observable at forward angles  $\theta < 70^\circ$ . It should be emphasized that there are no free parameters for the scattering problem in this simple model. The effective meson-nucleon coupling constants  $g_\sigma$  and  $g_\omega$  are determined by the ground state properties. It may indicate that the scattering properties of a nucleon from

the nucleus are mainly described by the ground state properties of the target nucleus in the energy region below 300 MeV. The target nuclei keep their ground state properties without being disturbed even at the incident energies of several hundred MeV. It was studied [4] that the mean field approximation based on the Walecka's model could describe the ground state properties of finite nuclei quite well, such as the single particle levels, charge and density distributions and so on. Our results also show that the RMOP based on the Walecka's model are adequate for describing the elastic scattering of a nucleon from a variety of spherical nuclei in a large energy region of  $E_p < 300$  MeV. It also indicates that the effective Lagrangian determined by ground state properties can describe both the ground state and the low lying state properties and the problem of the scattering of single particle for  $E_p < 300$  MeV. This model may be used in the nuclear transport theory and heavy ion collision and to take account of both the nuclear medium and relativistic effects.

It should be pointed out here that Yamaguchi et al. [11] have systematically analyzed the elastic proton scattering data for energies of 65 MeV to 200 MeV by using the nucleon-nucleus effective interactions in the framework of the nonrelativistic Brueckner-Hartree-Fock approximation and good agreement with the experiments is obtained. But the optical potentials given in Ref. 12 are calculated in the lowest order approximation based on the effective Skyrme interaction and are only adequate to the scattering at energies below several tens of MeV. Recently there have been some investigations of the RMOP in the framework of the relativistic Brueckner-Hartree-Fock approximation [13], but the applications of the theory to the analyses of the experimental data have not been seen in literature. However, direct evidence of the relativistic effects in the nucleon scattering for  $E < 300$  MeV cannot be concluded from our investigation in this paper.

## REFERENCES

- [1] Ma Zhongyu et al., p.171, Proc. of Beijing International Symp. on "Physics at Tandem", Beijing, China, May 26-30, 1986.  
Ma Zhongyu et al., submitted to Nucl. Phys.
- [2] J. A. McNeil, J. Shepard and S. J. Wallace, Phys. Rev. Lett. 50 (1983) 1439,  
J. Shepard, J. A. McNeil and S. J. Wallace, Phys. Rev. Lett. 50 (1983) 1443.
- [3] B. C. Clark et al., Phys. Rev. Lett. 50 (1983) 1644.
- [4] B. D. Serot and J. D. Walecka, Adv. in Nucl. Phys. 16 (1985) 1, eds. J. W. Negele, and E. Vogt (Plenum Press).
- [5] J. W. Negele, Phys. Rev. C1 (1970) 1260.
- [6] H. F. Ehrenberg et al., Phys. Rev. 113 (1959) 666.
- [7] H. Sakaguchi et al., J. Phys. Soc. Jpn. Suppl. 55 (1986) 61.
- [8] B. W. Ridley and J. F. Turner, Nucl. Phys. 58 (1964) 497,  
L. N. Blumberg et al., Phys. Rev. 147 (1966) 812,  
C. B. Folmer et al., Phys. Rev. 181 (1969) 1565,  
A. Johansson et al., Ark. Fys., 19 (1961) 541,  
A. Nadasen et al., Phys. Rev. C23 (1981) 1023.
- [9] H. Sakaguchi, Private communication.

- [10] B. C. Clark, Invited talk presented at the Los Alamos Workshop on Relativistic Dynamics and Quark-Nucleon Physics, June 2-14, 1985.
- [11] N. Yamaguchi et al., *Prog. of Theor. Phys.* 76 (1986) 1289.
- [12] Zhuo Yizhong et al., *Adv. of Chinese Sci. Phys.* 1 (1986) 231.